J|A|C|S
ARTICLES
Published on Web 03/17/2005

A Diameter-Selective Attack of Metallic Carbon Nanotubes by Nitronium Ions

Kay Hyeok An,[†] Jin Sung Park,[†] Cheol-Min Yang,[†] Seung Yol Jeong,[†] Seong Chu Lim,[†] Chul Kang,[‡] Joo-Hiuk Son,[‡] Mun Seok Jeong,[§] and Young Hee Lee*,[†]

Contribution from the BK21 Physics Division, Institute of Basic Science, Center for Nanotubes and Nanostructured Composites, Sungkyunkwan University, Suwon 440-746, Korea, Department of Physics, University of Seoul, Seoul 130-743, Korea, and Advanced Photonics Research Institute, Gwangju Institute of Science and Technology, Gwangju 500-712, Korea

Received November 30, 2004; E-mail: leeyoung@skku.edu

Abstract: We have found a method for a diameter-selective removal of metallic single-walled carbon nanotubes (m-SWCNTs) from semiconducting (s-) ones by stirring or sonicating SWCNT powder in tetramethylene sulfone (TMS)/chloroform solution with nitronium hexafluoroantimonate (NO_2SbF_6: NHFA) and nitronium tetrafluoroborate (NO_2BF_4: NTFB). Positively charged nitronium ions (NO_2^+) were intercalated into nanotube bundles, where the intercalation was promoted also by the counterions. Nitronium ions selectively attacked the sidewall of the m-SWCNTs due to the abundant presence of electron density at the Fermi level, thus yielding stronger binding energy as compared to the counterpart s-SWCNTs. The s-SWCNTs were left on the filter after filtration, whereas the m-SWCNTs were disintegrated and drained away as amorphous carbons. The effectiveness of removing m-SWCNTs was confirmed by the resonant Raman spectra and absorption spectra.

I. Introduction

Carbon nanotube is an emerging material for the realization of nanoscale devices in nanoscience and nanotechnology. The present state of the art technology for carbon nanotube synthesis always produced samples with mixing chiralities. The coexistence of metallic (m-SWCNTs) and semiconducting single-walled carbon nanotubes (s-SWCNTs) in commercially available samples has been a bottleneck for many fundamental researches and applications with high device performance, such as nanotransistors, memory devices, and chemical/bio-nanosensors. Several methods of separating semiconducting nanotubes from metallic ones or vice versa using dielectrophoresis, octadecylamine (ODA), bromination, and DNA have been reported.[1−5] Dielectrophoresis method requires a priori nanodispersion of nanotubes for high yield of separation and may not be scalable to large quantity. Preferential adsorption of ODAs on semiconducting nanotubes can give rise to high separation yield with large quantity, but extra work is necessary to remove additives. Bromination approach is easy and straightforward to understand but leaves a poor separation yield. Therefore, a realistic separation method for high yield and massive quantities of specific metallicity is still lacking.

Another approach is the functionalization that leads to transformation of the electronic structures of nanotubes. Strong chemisorption by hydrogenation and fluorination transformed electronic structures from m-SWCNTs to s-SWCNTs by inducing a partial sp^3 hybridization.[6,7] This sometimes deteriorated the nanotube walls, leading to a disintegration into amorphous carbons or graphitic layered structures.[8] The diazonium salts have been also introduced to react with the nanotubes to extract electrons from nanotubes in the formation of a covalent aryl bond, demonstrating chemoselective reactions with metallic versus the semiconducting nanotubes.[9] Thermal annealing of the diazonium-treated nanotubes at 300 °C cleaved the aryl moieties from the sidewalls and recovered the spectroscopic signatures of the pristine nanotubes. Small-diameter nanotubes have been selectively removed by an oxidative etching particularly with an assistance of light illumination.[10,11]

[†] Sungkyunkwan University.
[‡] University of Seoul.
[§] Advanced Photonics Research Institute.

(1) Krupke, R.; Hennrich, F.; Löhneysen, H. V.; Manfred, M.; Kappes, M. M. *Science* **2003**, *301*, 344−347.
(2) Zheng, M.; Jagota, A.; Strano, M. S.; Santos, A. P.; Barone, P.; Chou, S. G.; Diner, B. A.; Dresselhaus, M. S.; Mclean, R. S.; Onoa, G. B.; Samsonidze, G. G.; Semke, E. D.; Usrey, M.; Walls, D. J. *Science* **2003**, *302*, 1545−1548.
(3) Chattopadhyay, D.; Galeska, I.; Papadimitrakopoulos, F. *J. Am. Chem. Soc.* **2003**, *125*, 3370−3375.
(4) Chen, Z.; Du, X.; Rancken, C. D.; Cheng, H.-P.; Rinzler, A. G. *Nano Lett.* **2003**, *3*, 1245−1249.
(5) Samsonidze, G. G.; Chou, S. G.; Santos, A. P.; Brar, V. W.; Dresselhaus, M. S.; Selbst, A.; Swan, A. K.; Unlu, M. S.; Goldberg, B. B.; Chattopadhyay, D.; Kim, S. N.; Papadimitrakopoulos, F. *Appl. Phys. Lett.* **2004**, *85*, 1006−1008.
(6) Kim, K. S.; Bae, D. J.; Kim, J. R.; Park, K. A.; Lim, S. C.; Kim, J.-J.; Choi, W. B.; Park, C. Y.; Lee, Y. H. *Adv. Mater.* **2002**, *14*, 1818−1821.
(7) An, K. H.; Heo, J. G.; Jeon, K. G.; Bae, D. J.; Jo, C.; Yang, C. W.; Park, C.-Y.; Lee, Y. H. *Appl. Phys. Lett.* **2002**, *80*, 4235−4237.
(8) An, K. H.; Park, K. A.; Heo, J. G.; Jeon, Lim, S. C.; Yang, C. W.; Lee, Y. S.; Lee, Y. H. *J. Am. Chem. Soc.* **2003**, *125*, 3057−3061.
(9) Strano, M. S.; Dyke, C. A.; Usrey, M. L.; Barone, P. W.; Allen, M. J.; Shan, H.; Kittrell, C.; Hauge, R. H.; Tour, J. M.; Smalley, R. E. *Science* **2003**, *301*, 1519−1522.

10.1021/ja0428199 CCC: $30.25

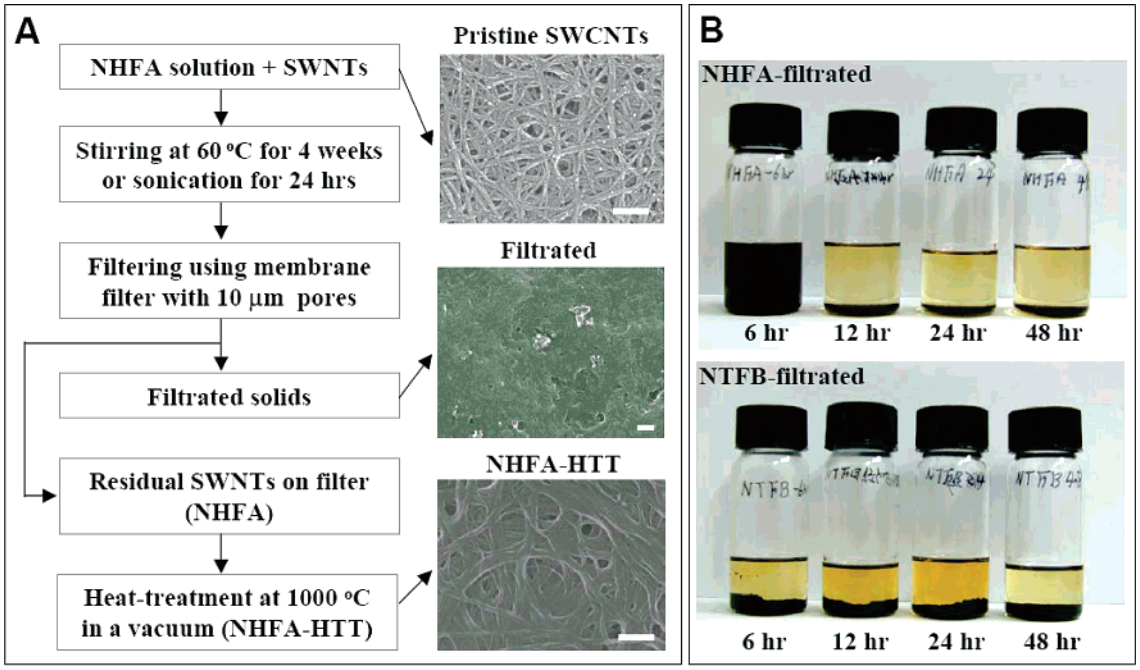

Figure 1. (A) Schematic representations of the NHFA and NTFB treatments of the HiPCO SWCNTs and their morphology changes of the pristine sample, the filtrated one at the bottom, and the residual SWCNTs on the filter after heat treatment (indicated as NHFA-HTT) from the top panel. The scale bar is 200 nm. (B) Photographs of the filtrated solids as a function of NHFA and NTFB treatment time.

Our aim is to select semiconducting nanotubes from metallic ones in a large quantity with high yield and more importantly without affecting nanotube properties so that the selected nanotubes could be utilized directly for various applications. Here, we report a new method of removing small-diameter m-SWCNTs from s-SWCNTs by dispersing SWCNT powder in tetramethylene sulfone (TMS)/chloroform solution with nitronium ions (NO_2^+). This method is simple and straightforward without altering electronic structures after treatment, and furthermore it is easily scalable for the large quantity of SWCNTs with high separation yield.

II. Experimental Section

Nitronium hexafluoroantimonate (NO_2SbF_6: NHFA) or nitronium tetrafluoroborate (NO_2BF_4: NTFB) of 50 mmol was dissolved in TMS/chloroform (1:1 by weight) solution of 100 mL. The nitronium salts were ionized in the mixed solvent as follows,

$$NO_2SbF_6 \rightarrow NO_2^+ + SbF_6^- \quad \text{or} \quad NO_2BF_4 \rightarrow NO_2^+ + BF_4^-$$

where both reactions produced nitronium ions.

The pristine HiPCO SWCNT soot of 10 mg purchased from CNI (Carbon Nanotechnologies Inc.) was suspended by either stirring for 4 weeks or sonicating for 24 h in the prepared NHFA or NTFB solution at 60 °C under N_2 bubbling. After reaction, the suspension was filtered using a membrane filter with a pore diameter of 10 μm and then washed with ethanol several times. The residual SWCNTs on the filter treated with NHFA or NTFB solution were dried in a vacuum at 100 °C for overnight, and further heat-treated in a vacuum at 1000 °C for 30 min. Figure 1A shows the sequence of procedures for the sample treatment.

The metallicity of samples was characterized by the resonant Raman spectroscopy (Renishaw, microprobe RM1000) with several wavelengths of 514.5 nm (Ar^+ ion laser), 632.8 nm (He−Ne laser), and 785 nm (diode laser). Samples were further analyzed by the field-emission scanning electron microscope (FESEM; JEOL 6700F). X-ray photoemission spectroscopy (XPS) was carried out using a PHI 5100 spectrometer using Mg Kα (1253.6 eV) line. The SWCNT powder was immersed in 2-propanol solution and sonicated for dispersion for 4 h. The absorption spectra were obtained by dropping a solution on a quartz plate using a UV−vis−NIR spectrophotometer (Hitachi U-3501).

III. Results and Discussion

Figure 1A shows the FESEM images of the pristine SWCNTs, filtrated solids, and NHFA-treated SWCNTs. The bundle size of the residual SWCNTs on the filter was enlarged due to an aggregation effect in solution without a distinct deformation of the nanotube walls. On the other hand, the morphology of the filtrated solid appeared somehow completely different from that of the pristine SWCNTs. The SWCNTs were hardly seen and mostly fragmented into small pieces, forming carbonaceous particles. Figure 1B demonstrates photographs of the filtrated solids during the filtering procedure as a function of NHFA and NTFB treatment times. The NHFA-treated sample at 6 h was well dispersed, while those at longer treatment time were precipitated at the bottom of the vial. The dispersed pristine SWCNTs in TMS/chloroform without NHFA or NTFB have not been filtrated through a membrane filter with a pore diameter of 10 μm. Therefore, we emphasized that the only nanotubes disintegrated by the NHFA were filtrated through the filter. Similar trends were observed with the NTFB treatment. It has been well known that the graphite surface can be attacked easily by nitronium ions at the graphite surface.[12] The nitronium ions capture the available π electrons in the (metallic) graphite, enhancing the binding energy with graphite surface. Because the SWCNTs have also similar π electrons on the surface except the strain effect, we expect that the nitronium ions can attack π electrons on the nanotube wall and thus provoke stable adsorption. The availability of the electrons at the Fermi level

(10) Yudasaka, M.; Zhang, M.; Iijima, S. *Chem. Phys. Lett.* **2003**, *374*, 132−136.
(11) Banerjee, S.; Wong, S. S. *Nano Lett.* **2004**, *4*, 1445−1450.
(12) Forsman, W. C.; Mertwoy, H. E. *Synth. Met.* **1980**, *2*, 171−176.

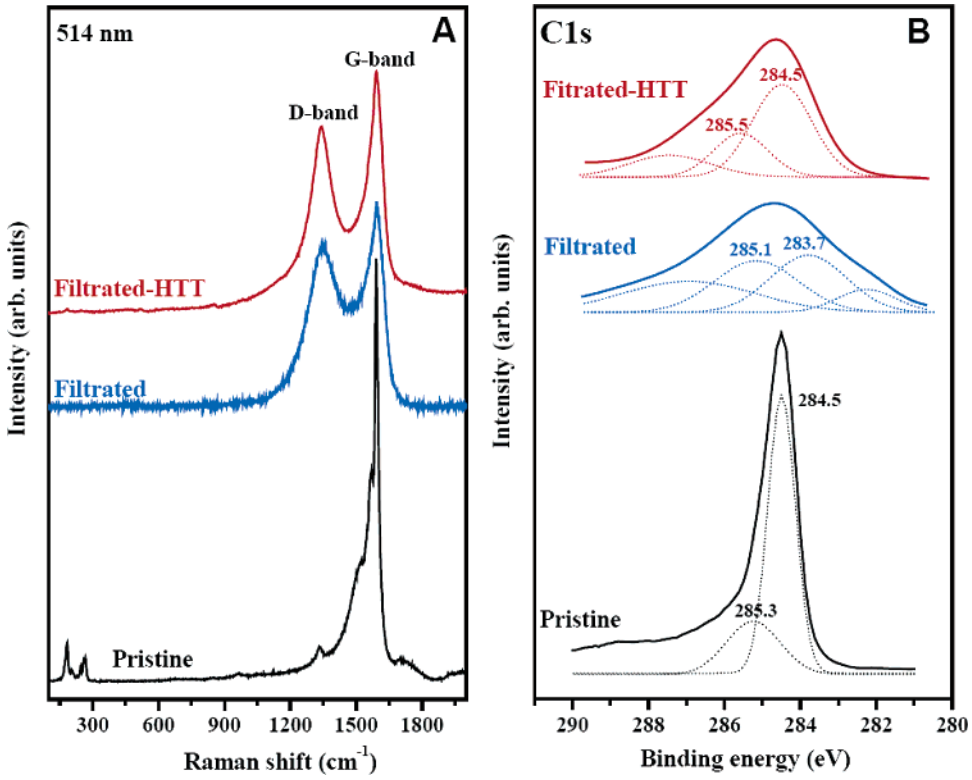

Figure 2. Raman spectra (A) and XPS spectra (B) of the pristine sample, the filtrated solid, and the heat-treated filtrated solid at 1000 °C in a vacuum.

is a key factor in determining the binding nature, similar to the diazonium effect.[9] Because the m-SWCNTs have more abundant electron charge density at the Fermi level than the counterpart s-SWCNTs, we expect that nitronium ions can be adsorbed more strongly on m-SWCNT sidewalls than on s-SWCNT ones. Strong adsorption of nitronium ions may attack the m-SWCNT sidewalls and furthermore disintegrate the nanotube walls, as observed in our experiments.

The disintegrated m-SWCNTs by an attack of nitronium ions during NHFA treatment were filtrated out during the filtering process. Figure 2A shows the Raman spectra of the filtrated solids at the excitation energy of 514 nm. The pristine sample clearly reveals the G-band near 1590 cm^{-1}, small D-band near 1330 cm^{-1}, and the radial breathing modes (RBMs) near 100−300 cm^{-1}, demonstrating a typical behavior of SWCNTs. In good contrast with this, the D-band of the filtrated sample, which is a characteristic of amorphous carbons or defects, increased drastically, while the RBM peaks near 100−300 cm^{-1} were completely disappeared. After heat treatment at 1000 °C, the ratio of D-band to G-band was not reduced, and furthermore the RBM modes were not recovered. The XPS C1s spectra of the pristine sample in Figure 2B show two characteristic peaks near 284.5 eV, sp^2-hybridized or graphitic carbons, and 285.3 eV, sp^3-hybridized or defective carbons.[13] This peak became broadened after NHFA treatment, and furthermore the ratio of sp^3-like bonds to sp^2-like bonds was significantly increased. The broad peak near 287.5 eV and the small peak near 282 eV (carbidic carbon)[14] together with the broadened main peaks indicated the filtrated solids to be functionalized by various adsorbates. The broad peak was still maintained after heat treatment, although the intensity of the graphitic peak was increased due to the crystallization effect. These lead to the conclusion that the filtrated SWCNTs were disintegrated into amorphous carbons, in good agreement with the SEM morphology for the precipitated solids (Figure 1A). Interestingly, the amount of the sample loss after filtration was about 25−30 wt %, close to the theoretically estimated metallic content. Similar results were obtained with NTFB treatment, although the reactivity was less effective. This implies that the anion plays an important role during reaction as an intercalator into the bundle. The anion size (SbF_6^-) of the NHFA is larger than BF_4^- of NTFB, providing more rooms for nitronium ions to be intercalated into the bundle.

To clarify the nature of metallicity of the residual sample on the filter, we investigated the resonant Raman spectra. The SWCNTs were drop-casted on quarts substrate. The numbers in Figure 3 indicate the corresponding diameters from each peak determined by [ω (cm^{-1}) = 235/d (nm) + 9].[15] The metallic and semiconducting bands indicated by the dotted square boxes were determined from the Kataura plot.[16] We identified five distinct peaks in the RBM mode from the pristine sample at an excitation energy of 514 nm in Figure 3A. The RBM bands can be grouped into two characters: semiconducting S_{33} band (183 and 204 cm^{-1}) and metallic M_{11} band (244, 259, and 266 cm^{-1}). Interestingly, the metallic band was completely removed after NHFA treatment, whereas the semiconducting peaks were slightly upshifted. This implies that nitronium ions could be adsorbed even on s-SWCNTs so as to upshift the peak positions

(13) Choi, H. C.; Kim, S. Y.; Jang, W. S.; Bae, S. Y.; Park, J.; Kim, K. L.; Kim, K. *Chem. Phys. Lett.* **2004**, *399*, 255−259.
(14) Biniak, S.; Szymański, G.; Siedlewski, J.; Światkowski, A. *Carbon* **1997**, *35*, 1799−1810.
(15) Kuzmany, H.; Plank, W.; Hulman, M.; Kramberger, C.; Gruneis, A.; Pichler, T.; Perterlik, H.; Achiba, Y. *Eur. Phys. J. B* **2001**, *22*, 307.
(16) Kataura, H.; Kumaza, Y.; Maniwa, Y.; Umezu, I.; Suzuki, S.; Ohtsuka, Y.; Achiba, Y. *Synth. Met.* **1999**, *103*, 2555−2558.

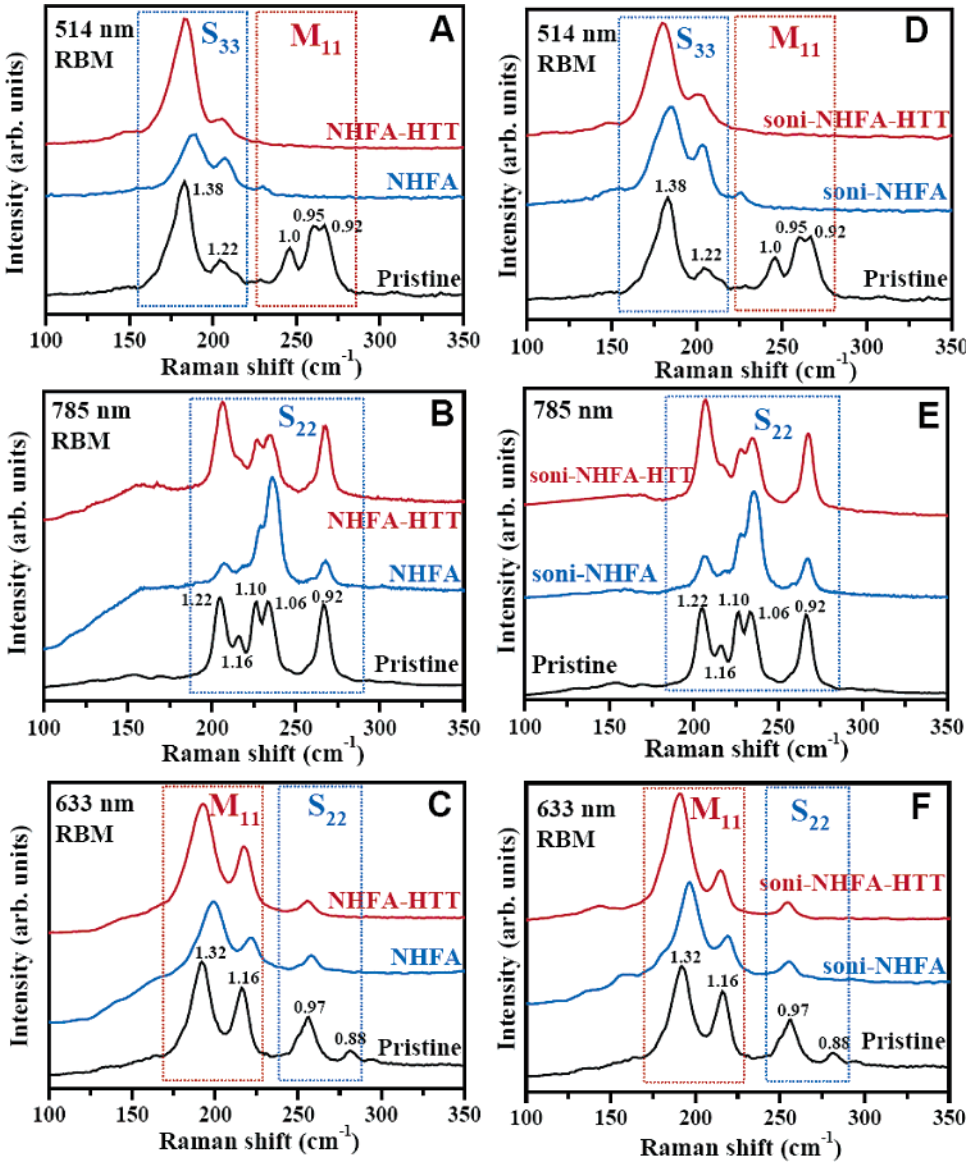

Figure 3. RBMs of Raman spectra with excitation energies of 514 nm (A, D), 785 nm (B, E), and 633 nm (C, F) for the pristine sample, the residual sample on the filter after the NHFA treatment by either stirring for 4 weeks (NHFA) or sonicating for 24 h (soni-NHFA), and the residual sample with further heat treatment at 1000 °C (NHFA-HTT or soni-NHFA-HTT) in a vacuum.

due to the charge transfer to the nitronium ions, similar to an acceptor behavior.[7] After heat treatment at 1000 °C in a vacuum, the peak shift of the semiconducting band was recovered and the peak was intensified. All of the adsorbates were removed after heat treatment, which will be discussed later in the XPS analysis. However, the metallic band was still not visible. Therefore, the disappearance of the metallic band was not due to the shift of the resonance, in good contrast with the previous works that the disappeared band in the RBM by the diazonium adsorption was recovered simply due to the desorption after heat treatment, leaving unaltered electronic structures of nanotubes. [9,17]

Figure 3B shows the RBM profiles at an excitation energy of 785 nm. In this case, we observed only the semiconducting S_{22} band (205, 216, 226, 234, and 267 cm^{-1}) from the pristine sample. The peak intensities of the large (1.22 nm)- and small (0.92 nm)-diameter nanotubes were reduced, and the peak positions were slightly upshifted after NHFA treatment. The large-diameter nanotubes form a rather large interstitial space in the bundle to provide better accessibility for adsorbates.[18−20] On the other hand, in small-diameter nanotubes, the ratio of adsorbate to nanotube is high, and furthermore large strain induces strong binding energy with adsorbates.[18−20] This provokes one to violate the resonance condition and shifts the peak positions. The related peak intensities were reduced as shown in the figure. These peaks were fully recovered again with similar intensity ratios and peak positions after heat treatment. The binding energy of nitronium ions to the sidewall of the semiconducting nanotubes was not strong enough to destroy nanotubes during adsorption and desorption, such that the electronic structures of s-SWCNTs remained unchanged after

(17) An, L.; Fu, Q.; Lu, C.; Liu, J. *J. Am. Chem. Soc.* **2004**, *126*, 10520−10521.
(18) Kukovecz, A.; Pichler, T.; Pfeiffer, R.; Kuzmany, H. *Chem. Commun.* **2002**, 1730−1731.
(19) Kukovecz, A.; Pichler, T.; Kramberger, C.; Kuzmany, H. *Chem. Commun.* **2003**, *5*, 582−587.
(20) Kavan, L.; Dunsxh, L. *Nano Lett.* **2003**, *3*, 969−972.

heat treatment. We emphasize here that s-SWCNTs with small diameters of 0.92 nm were not disintegrated after treatments, whereas the corresponding metallic band with diameters less than 1.1 nm was completely removed in Figure 3A. This strongly suggests that the nitronium ions attacked selectively the m-SWCNTs with small diameters less than 1.1 nm.

We also observed the Raman spectra with an excitation energy of 633 nm, as shown in Figure 3C. In this case, the metallic bands at 216 cm^{-1} (1.16 nm) and 192 cm^{-1} (1.32 nm) and the semiconducting bands at 256 cm^{-1} (0.97 nm) and 281 cm^{-1} (0.88 nm) appeared in the pristine sample. The small-diameter (0.97 nm) s-SWCNTs were attacked to lead to a partial disintegration after NHFA and heat treatments, which is in good contrast with the completely recovered semiconducting peak of 0.92 nm at 785 nm. The semiconducting peak at 281 cm^{-1} (0.88 nm) was completely disappeared. The strain is too large, 0.12 eV/atom in this case,[21] such that nanotubes can be disintegrated independent of the metallicity. The metallic band was upshifted with NHFA treatment, confirming again an adsorption of nitronium ions, and was recovered again after heat treatment, similar to the semiconducting one in Figure 3B. Yet, the preferable binding energy on m-SWCNTs to that of s-SWCNTs was not large enough to disintegrate m-SWCNTs, as predicted from theoretical calculations.[22] The selective attack of metallic nanotubes became unclear at nanotubes with diameters of greater than 1.1 nm. This inconsistent result may originate from the inhomogeneous distribution of nanotubes with different diameters in the bundle. Similar phenomena were also observed in ODA-treated samples.[5] Instead of having a long stirring time of 4 weeks, we also tried a short treatment time of 24 h with sonication. The effects were very similar, as shown in Figure 3D−F. The sonication approach seemed to be more effective in removing large-diameter m-SWCNTs, as shown in Figure 3F. The sonication generally gives a better dispersion of nanotubes and thus promotes the reaction of nanotubes with adsorbates.

So far, we learned that the selective disintegration of m-SWCNTs is diameter-dependent. In small-diameter nanotubes of less than 1.1 nm, both the strain effect and the abundance of charge density at the Fermi level play a dominant role for a selective removal of metallic nanotubes. However, at large-diameter nanotubes of greater than 1.1 nm, the strain effect may be excluded. This strongly suggests that the selective adsorption on metallic nanotubes can be achieved by the abundant presence of charge density at the Fermi level and the extra strain effect should be accommodated to destroy the nanotube walls.

The selective removal of metallic nanotubes can be also revealed from the G-band analysis. The G-band was fitted with four semiconducting Lorentzian lines and two metallic components (red).[23] The long tail at a lower energy side of the G-band is a characteristic of the metallic component and should be fitted by the Breit−Wigner−Fano (BWF) line shape. The two metallic components (red) were clearly observed in the pristine sample (Figure 4A). These two metallic components completely disappeared in the NHFA-treated sample (Figure 4B), whereas the semiconducting peaks remained almost

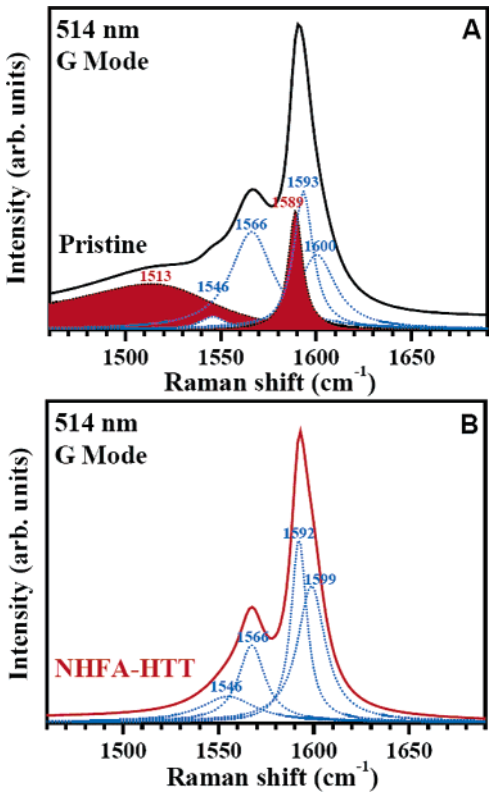

Figure 4. (A) The curve fitting of the tangential mode at 514 nm with four semiconducting Lorentzian shapes and two metallic BWF line shapes (red color) for the pristine sample. (B) The similar curve fitting but with four semiconducting Lorentzian shapes only for the NHFA-treated sample for 4 weeks followed by the heat treatment at 1000 °C in a vacuum.

unchanged. This again indicates a selective destruction of metallic nanotubes.

The selective disintegration of m-SWCNTs involves strong chemisorption with nitronium ions. The evidence of chemisorption of nitronium ions to the sidewall of m-SWCNTs was observed in X- ray photoemission spectroscopy (XPS) data. The C1s XPS spectrum of the pristine SWCNTs showed two components (Figure 5A). The peak around 284.5 eV represented sp^2-hybridized carbons on the tube wall, which is comparable to the C1s binding energy of graphite. The small peak around 285.3 eV was related to sp^3-hybridized carbons that may originate from the presence of defects on the tube walls.[13] After NHFA treatment, these peaks were broadened and downshifted by about 1 eV, indicating a strong charge transfer on adsorbates that was provoked between nanotubes and nitronium ions during adsorption. This shift was completely recovered with full width at half-maximum similar to that of the pristine sample after heat treatment. In addition, three small peaks were newly developed at 285.4, 287.4, and 288.3 eV, which were assigned to C−N, C═O, and C−F bonds, respectively.[7,13,24] These peaks disappeared after heat treatment. In the O1s XPS spectrum of the pristine SWCNTs, the presence of ambient oxygen species was observed in Figure 5B. The oxygen-related peaks were heavily developed with NHFA treatment due to the abundant adsorption of nitronium ions, which were again significantly reduced with heat treatment. Similar behavior was also observed with N1s and F1s spectra. The C−N related and N−O related peaks were

(21) Oh, D.-H.; Lee, Y. H. *Phys. Rev. B* **1998**, *58*, 7407−7411.
(22) Seo, K.; Kim, C.; Park, K. A.; Han, S.; Kim, B.; Lee, Y. H. unpublished.
(23) Brown, S. D. M.; Jorio, A.; Corio, P.; Dresselhaus, M. S.; Dresselhaus, G.; Saito, R.; Kneipp, K. *Phys. Rev. B* **2000**, *63*, 155414.
(24) Okpalugo, T. I. T.; Papakonstantinou, P.; Murphy, H.; McLaughlin, J.; Brown, N. M. D. *Carbon* **2004**, *43*, 153−161

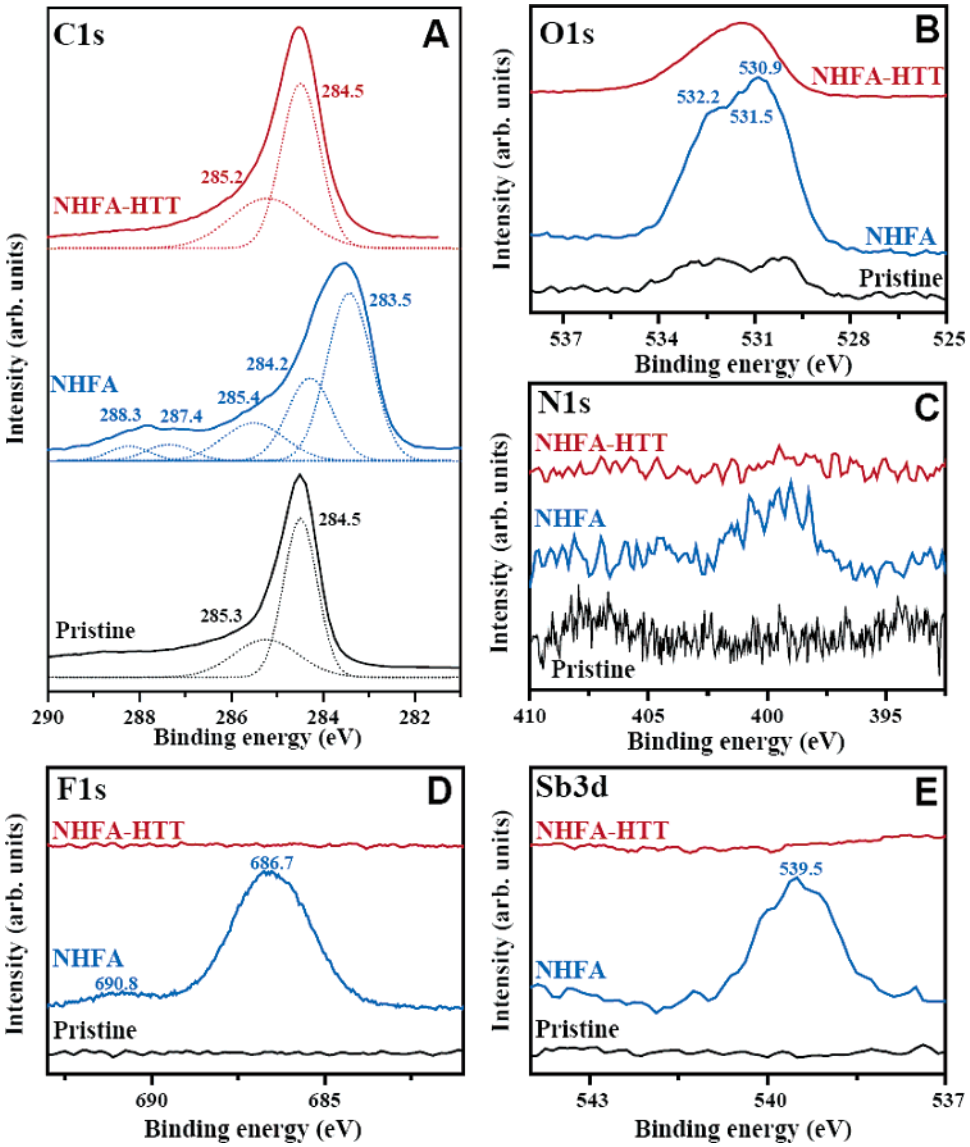

Figure 5. XPS spectra of C1s with Gaussian curve fittings (A), O1s (B), N1s (C), F1s (D), and Sb3d (E) for the pristine sample, NHFA-treated one, and NHFA-HTT, respectively.

observed near 402.5−396.5 eV from N1s spectra (Figure 5C).[14] Ionic C−F bonds near 686.7 eV were heavily developed with small covalent peaks near 690.8 eV in the NHFA-treated sample (Figure 5D).[25] The disappearance of these peaks after heat treatment concurred with C1s spectra. We also observed the SbO_x-related peak near 539.5 eV in the NHFA-treated sample due to intercalation of hexafluoroantimonate ions into the SWCNT bundles.[26] Yet SbO_x-related materials were also removed during heat treatment, as shown in Figure 5E.

Terahertz (THz) conductivity measurements of SWCNT films on quartz substrate were performed to further prove the selective separation of s-SWCNTs. The dynamic response of the electrical conductivity for SWCNT films was measured using terahertz time-domain spectroscopy (THz-TDS) in the frequency range of 0.2−2.0 THz. THz-TDS is based on the optoelectronic generation and detection of a beam of subpicosecond THz pulses.[27,28] The real conductivity as a function of THz was calculated from the measured index of refraction and power absorption as a function of THz.[29] Figure 6A shows the real conductivities of the pristine and NHFA-treated SWCNTs as a function of THz frequency. The conductivities of both samples decreased with increasing frequency at the high-frequency region, following a simple Drude model, except not in the low-frequency region. This behavior has been explained by the influence of phonon absorption along the tube axis of s-SWCNTs.[27,28] What is more intriguing is that the real conductivity of the NHFA-treated SWCNTs was reduced by about 25−30% consistently over all frequency ranges as compared to that of the pristine SWCNTs. Interestingly, the relative percentage of the conductivity reduction was close to that of the weight reduction observed during NHFA treatment. This reflects again the selective removal of m-SWCNTs, in agreement with Raman data.

(25) Hayashi, T. *Nano Lett.* **2004**, *4*, 1001.
(26) Zeng, D. W.; Zhu, B. L.; Xie, C. S.; Song, W. L.; Wang, A. H. *Mater. Sci. Eng.* **2004**, *A366*, 332−337.
(27) Jeon, T.-I.; Kim, K.-J.; Kang, C.; Oh, S.-J.; Son, J.-H.; An, K. H.; Bae, D. J.; Lee, Y. H. *Appl. Phys. Lett.* **2002**, *80*, 3403−3405.
(28) Jeon, T.-I.; Kim, K.-J.; Kang, C.; Oh, S.-J.; Son, J.-H.; An, K. H.; Lee, J. Y.; Lee, Y. H. *J. Appl. Phys.* **2004**, *95*, 5736−5740.

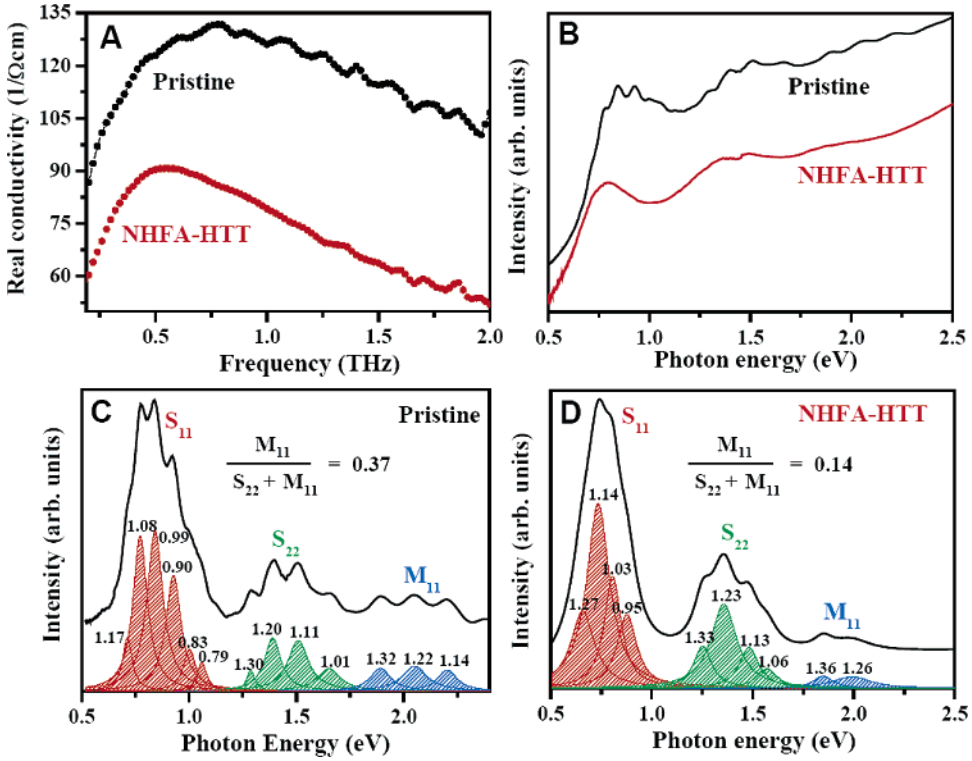

Figure 6. (A) THz time-domain spectroscopy of the pristine sample and the NHFA-HTT sample and (B) the corresponding optical absorption spectra in the visible range. (C), (D) The Lorentzian curve fitting of each band for the pristine sample and the NHFA-HTT sample. The baselines were subtracted from the background plasmons for the curve fitting. Values in the figure were the corresponding diameters of each curve determined from the tight-binding model.

The absorption spectra in the infrared and visible ranges can provide information for the metallicity of the whole sample, which cannot be obtained practically from resonant Raman data. It is well established that the optical response of SWCNTs is dominated by transitions between peaks in the electronic density of states, with momentum conservation only allowing transition pairs of van Hove singularities with a mirror symmetry to the Fermi level.[30−32] Furthermore, the widths and fine structures of these absorption bands are specifically related to the distribution of diameters and chiralities of nanotubes.[33,34] The optical absorption spectra of the pristine and NHFA-treated SWCNTs were compared in Figure 6B to distinguish the metallicity between two samples. In the pristine SWCNTs, transitions between the first and second van Hove singularities (S_{11} and S_{22}) in s-SWCNTs were observed near 0.9 eV (S_{11}) and 1.5 eV (S_{22}), whereas the related peak (M_{11}) in m-SWCNT was observed near 2.0 eV. Although the nanodispersion of the pristine SWCNTs was insufficient in isopropyl alcohol followed by a drop casting on quartz substrate, several subband peaks in each band were clearly visible. On the other hand, several subband peaks in the NHFA-treated SWCNTs were suppressed due to the formation of large bundles during NHFA treatment, as shown in Figure 1A. We note that the intensity of the M_{11} transition peak of the NHFA-treated SWCNTs was greatly suppressed due to the selective removal of m-SWCNTs. Moreover, the transition energies of the semiconducting peaks were all downshifted, suggesting that even for semiconducting nanotubes, some portions of the small diameter s-SWCNTs were also removed.

To determine the separation yield, we performed the curve fitting of the absorption spectra. The transition energy is inversely proportional to the tube diameter.[35,36] The diameter distribution, which is written on the fitted curves in Figure 6C and D, clearly demonstrated the removal of small-diameter SWCNTs by the NHFA treatment. The small amount of M_{11} transitions at the lower energy side (large diameter) still remained in the sample even after NHFA treatment. We note that the semiconducting nanotubes with small diameters near 0.95 and 1.03 nm were still visible in the NHFA-treated sample. These changes were in good agreement with the Raman data. The previous theoretical calculations demonstrated that the NO_2 binding energy with the metallic nanotube was stronger than that with the semiconducting nanotube due to large charge transfer and furthermore the binding energy of each chiral nanotube became weaker with increasing diameters.[22] The separation yield of the sample can be drawn by the ratio of S_{22} and M_{11} transitions in the optical absorption spectra. Because the S_{11} band might be modified more easily than the S_{22} band,[33] we extracted information of the separation yield from $M_{11}/(S_{22} + M_{11})$. This value was 0.37 from the pristine sample, close to the theoretical estimate. This was reduced to 0.14 after the NHFA treatment followed by thermal annealing. If one starts with small-diameter nanotubes of less than 1.1 nm, the yield of

(29) Duvilaret, L.; Garet, F.; Coutaz, J.-L. *IEEE J. Sel. Top. Quantum Electron.* **1996**, *2*, 739−746.
(30) Mintmire, J. W.; White, C. T. *Phys. Rew. Lett.* **1998**, *81*, 2506−2509.
(31) Saito, R.; Dresselhaus, G.; Dresselhaus, M. S. *Phys. Rev. B* **2000**, *61*, 2981−2990.
(32) Reich, S.; Thomsen, C. *Phys. Rev. B* **2000**, *62*, 4273−4276.
(33) Itkis, M. E.; Perea, D. E.; Niyogi, S.; Rickard, S. M.; Hamon, M. A.; Hu, H.; Zho, B.; Haddon, R. C. *Nano Lett.* **2003**, *3*, 309−314.
(34) Liu, X.; Pichler, T.; Knupfer, M.; Golden, M. S.; Fink, J.; Kataura, H.; Achiba, Y. *Phys. Rev. B* **2002**, *66*, 045411.

(35) $S_{11} = 2a_0\gamma_0/d$, $S_{22} = 4a_0\gamma_0/d$, and $M_{11} = 6a_0\gamma_0/d$, where a_0 is the carbon−carbon bond length (0.144 nm), γ_0 is the tight-binding parameter of the nearest neighbor overlap integral (2.9 ± 0.5 eV), and d is diameter in nanometers.

(36) Hamon, M. A.; Itkis, M. E.; Nigogi, S.; Alvaraez, T.; Kuper, C.; Menon, M.; Haddon, R. C. *J. Am. Chem. Soc.* **2001**, *123*, 11292−11293.

separation would be close to 100%. Our approach with nitronium ions in solvent is easily scalable to large quantity treatment, and moreover no additive is left in the sample without altering the electronic structures of nanotubes such that the separated nanotubes can be directly used for other purposes.

IV. Conclusions

We have investigated a liquid-phase reaction using nitronium ions to remove metallic carbon nanotubes. We presented a separation technique that is capable of removing metallic nanotubes at small diameters of less than 1.1 nm with high yield. The s-SWCNTs remained intact with NHFA treatment, while the m-SWCNTs were completely destroyed and removed, especially for nanotubes with diameters close to or less than 1.1 nm. The nitronium ion selectively adsorbed on m-SWCNTs with higher binding energy by inducing a stronger charge transfer from nanotube to nitronium ion. This is due to the higher availability of electron density at the Fermi level of the metallic nanotubes, as compared to the counterpart s-SWCNTs. This difference becomes obscured for nanotubes with diameters greater than 1.1 nm. Our approach is straightforward without altering electronic structures during the treatment and is easily scalable to a large quantity process.

Acknowledgment. This work was supported by the MOST through NRL program, New Frontier project, CNNC at SKKU, and Environmental Technology project of MOE.

JA0428199